

Free vibration analysis of moderately-thick and thick toroidal shells

X.H. Wang*¹ and D. Redekop²

¹Department of Civil Engineering, Shantou University, 243 Da Xue Road, Shantou, P.R. China

²Department of Mechanical Engineering, University of Ottawa, Ottawa, Canada K1N 6N5

(Received July 30, 2010, Accepted May 1, 2011)

Abstract. A free vibration analysis is made of a moderately-thick toroidal shell based on a shear deformation (Timoshenko-Mindlin) shell theory. This work represents an extension of earlier work by the authors which was based on a thin (Kirchoff-Love) shell theory. The analysis uses a modal approach in the circumferential direction, and numerical results are found using the differential quadrature method (DQM). The analysis is first developed for a shell of revolution of arbitrary meridian, and then specialized to a complete circular toroidal shell. A second analysis, based on the three-dimensional theory of elasticity, is presented to cover thick shells. The shear deformation theory is validated by comparing calculated results with previously published results for fifteen cases, found using thin shell theory, moderately-thick shell theory, and the theory of elasticity. Consistent agreement is observed in the comparison of different results. New frequency results are then given for moderately-thick and thick toroidal shells, considered to be completely free. The results indicate the usefulness of the shear deformation theory in determining natural frequencies for toroidal shells.

Keywords: vibration; toroidal shells; shear deformation theory; theory of elasticity; differential quadrature method

1. Introduction

Toroidal shells (Fig. 1) over the years have been proposed for, or used, in such applications as fusion reactor vessels, satellite support structures, protective devices for nuclear fuel containers, circumferential reinforcement for submarines, rocket fuel tanks, and diver's oxygen tanks. Vibration analyses are an important part of the design process for such applications. Analytical solutions are useful in vibration analyses, either in the form of a primary solution or as a means to supplement results determined using the finite element method (FEM).

There is extensive literature on the analysis of toroidal shell vibrations based on the classical (Kirchoff-Love) shell theory (Balderes and Armenakas 1973, Leung and Kwok 1994, Wang and Redekop 2005, Kosawada *et al.* 1985). This theory is restricted in validity to relatively thin shells. There is further literature on toroidal shell vibrations using theories applicable for thicker shells (Kosawada *et al.* 1986, Buchanan and Liu 2005, McGill and Lenzen 1967, Jiang and Redekop 2002). Among these is the work by Kosawada *et al.* (1986), who developed a solution for toroidal

*Corresponding author, Professor, E-mail: wangxh@stu.edu.cn

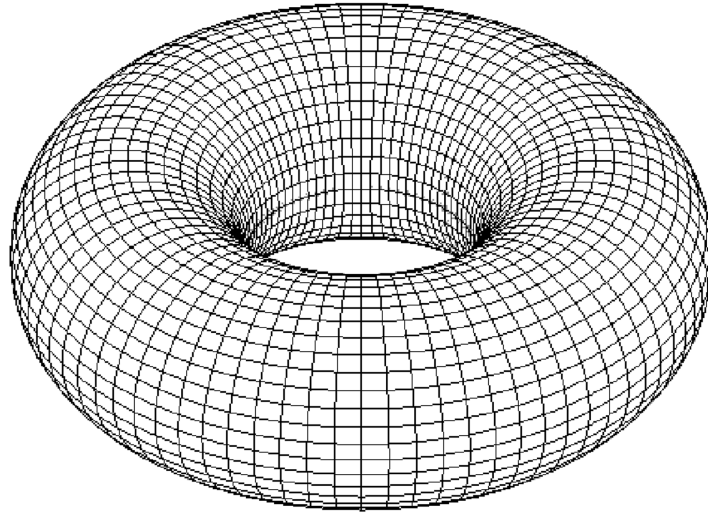


Fig. 1 Complete circular toroidal shell

shell vibrations based on a shear-deformation theory. However, this comprehensive work included an awkward series solution in the thickness direction, which required some calculations in quadruple precision. A collection of results for frequencies of vibrations of thin and thick toroidal shells, determined by either analytical or numerical methods, is given in Wang *et al.* (2006). A solution based on shear deformation theory has been presented recently for a shell of revolution (Artioli *et al.* 2005, Artioli and Viola 2006), but the application was intended for paraboloidal shells rather than toroidal ones. Analyses for thick toroidal shells to date have been based on the FEM (Buchanan and Liu 2005), or have dealt only with axi-symmetric vibrations (McGill and Lenzen 1967, Jiang and Redekop 2002). Certainly for some applications, toroidal shells will be moderately-thick or thick; it is desirable to establish effective theories appropriate for their analysis.

In this study, equations based on shear deformation (SDT) theory of Soedel (1982, 2004) are developed for the linear free vibration analysis of an isotropic homogeneous toroidal shell. The work can be considered an extension of the authors' previous work on thin toroidal shells (Wang and Redekop 2005). The equations are first written for a general shell, then specialized for a shell of revolution, and finally adapted for the circular toroidal geometry. A modal expansion is written in the circumferential direction, and equations are solved for each mode using the effective differential quadrature method (DQM). A second analysis, based on the theory of elasticity (ELT), is presented to cover shells of greater, arbitrary thickness. The SDT approach is validated by comparing results for complete thin, moderately-thick, and thick toroidal shells with previously published results. A parametric study is then conducted, covering moderately-thick and thick toroidal shells. An indication of the limiting range of application of the SDT is given. Conclusions are drawn about the usefulness of this theory for analyzing toroidal shell vibrations.

2. Geometry and boundary conditions

The mid-surface of an arbitrary shell (Soedel 2004) is described by a radius vector $\mathbf{R} = \mathbf{R}(q_1, q_2)$,

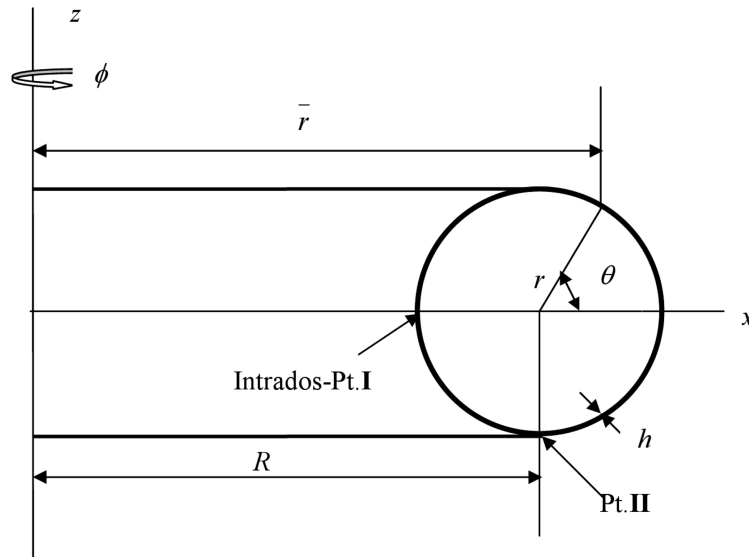


Fig. 2 Cross-sectional geometry of circular toroidal shell; point I is the intrados, point II is the lower crown

where q_1, q_2 form an orthogonal Gaussian coordinate system. For a shell of revolution, the radius vector takes the form $\mathbf{R} = \check{r}\sin\varphi\mathbf{i} + \check{r}\cos\varphi\mathbf{j} + z\mathbf{k}$, where $q_1 \equiv \varphi$ is the circumferential angle, $\check{r} = \check{r}(q_2)$, $z = z(q_2)$, and $\mathbf{i}, \mathbf{j}, \mathbf{k}$ are the Cartesian unit vectors.

The Lamé parameters of the shell are represented by A_1, A_2 , and the radii of curvatures by R_1, R_2 . For a toroidal shell of a circular cross-section, (Fig. 2) these four parameters are given (Soedel 2004) by

$$A_1 = R + r\cos\theta; \quad A_2 = r; \quad R_1 = (R + r\cos\theta)/\cos\theta; \quad R_2 = r \quad (1)$$

where $q_2 \equiv \theta$ is the meridional angle, measured clockwise from the positive horizontal, R is the bend radius, and r is the radius of the cross-section.

For a complete toroidal shell, the meridian forms a closed curve, and boundary conditions need not be considered if a shell theory is used. The present method can easily be extended to a toroidal shell with an incomplete meridian by specifying appropriate boundary conditions at the ends of the meridian of such a shell. In the application of the theory of elasticity, boundary conditions must be satisfied on the inner and outer surfaces to ensure zero traction conditions.

3. Shear deformation shell theory

The shear deformation theory presented by Soedel (1982, 2004) is adopted for this study. The assumptions of the theory correspond to those of the Timoshenko beam theory and the Mindlin plate theory, namely that the normal stress in the thickness direction is zero, and that a normal to the shell mid-surface remain straight, but not necessarily normal. The theory is presented here first for the linear behavior of general moderately thick shells consisting of elastic homogeneous isotropic materials.

In this theory, the mid-surface strains and changes of curvature are Soedel (1982, 2004)

$$\begin{aligned} \varepsilon_1 &= a_1 u_{1,1} + a_2 u_2 + a_3 u_3; & \varepsilon_2 &= a_4 u_1 + a_5 u_{2,2} + a_6 u_3; & \varepsilon_{12} &= a_7 u_{1,2} + a_8 u_1 + a_9 u_{2,1} + a_{10} u_2 \\ \kappa_1 &= a_{11} \beta_{1,1} + a_{12} \beta_2; & \kappa_2 &= a_{13} \beta_1 + a_{14} \beta_{2,2}; & \kappa_{12} &= a_{15} \beta_{1,2} + a_{16} \beta_1 + a_{17} \beta_{2,1} + a_{18} \beta_2 \end{aligned} \quad (2)$$

where u_1, u_2, u_3 are respectively the mid-surface displacements in the q_1, q_2 , and normal directions, β_1, β_2 are respectively the mid-surface rotations about the local q_2, q_1 directions, and the comma subscripts indicates differentiation with respect to the q_i number variable that follows. The transverse shear strains are given by

$$\varepsilon_{13} = a_{19} u_1 + a_{20} u_{3,1} + \beta_1; \quad \varepsilon_{23} = a_{21} u_2 + a_{22} u_{3,2} + \beta_2 \quad (3)$$

where the coefficients a_i in the expressions for the strain components and changes of curvature are defined in terms of the Lamé parameters and the radii of curvatures by

$$\begin{aligned} a_1 &= 1/A_1; & a_2 &= A_{1,2}/(A_1 A_2); & a_3 &= 1/R_1; & a_4 &= A_{2,1}/(A_1 A_2); & a_5 &= 1/A_2; & a_6 &= 1/R_2 \\ a_7 &= a_5; & a_8 &= -A_{1,2}/(A_1 A_2); & a_9 &= a_1; & a_{10} &= -a_4; & a_{11} &= a_1; & a_{12} &= a_2; & a_{13} &= a_4; & a_{14} &= a_5 \\ a_{15} &= a_5; & a_{16} &= -a_2; & a_{17} &= a_1; & a_{18} &= -a_4; & a_{19} &= -a_3; & a_{20} &= a_1; & a_{21} &= -a_6; & a_{22} &= a_5 \end{aligned} \quad (4)$$

The force and moment resultants are given by

$$\begin{aligned} N_1 &= b_1 \varepsilon_1 + b_2 \varepsilon_2; & N_2 &= b_3 \varepsilon_1 + b_4 \varepsilon_2; & N_{12} &= b_5 \varepsilon_{12} \\ M_1 &= b_6 \kappa_1 + b_7 \kappa_2; & M_2 &= b_8 \kappa_1 + b_9 \kappa_2; & M_{12} &= b_{10} \kappa_{12} \end{aligned} \quad (5)$$

while the transverse shear resultants by

$$Q_{13} = b_{11} u_1 + b_{12} u_{3,1} + b_{13} \beta_1; \quad Q_{23} = b_{14} u_2 + b_{15} u_{3,2} + b_{16} \beta_2 \quad (6)$$

The coefficients b_i are defined in terms of the material and geometric properties by

$$\begin{aligned} b_1 &= K; & b_2 &= \nu K; & b_3 &= b_2; & b_4 &= b_1; & b_5 &= (1-\nu)K/2; & b_6 &= D; & b_7 &= \nu D; & b_8 &= b_7 \\ b_9 &= b_6; & b_{10} &= (1-\nu)D/2; & b_{11} &= -k'Gh/R_1; & b_{12} &= -k'Gh/A_1; & b_{13} &= k'Gh \\ b_{14} &= -k'Gh/R_2; & b_{15} &= k'Gh/A_2; & b_{16} &= b_{13}; & b_{17} &= A_1 A_2 k'Gh; & b_{18} &= b_{13} \end{aligned} \quad (7)$$

where E is the Young's modulus, ν the Poisson's ratio, $2G = E/(1 + \nu)$, k' the shear factor (taken as $2/3$), h the shell wall thickness, $K = Eh/(1 - \nu^2)$, and $D = Kh^2/12$.

The equations of motions (Soedel 1982, 2004) are given by

$$c_1 N_{1,t} + c_2 N_1 + c_3 N_2 + c_4 N_{12,2} + c_5 N_{12} + c_6 u_1 + c_7 u_{3,1} + c_8 \beta_1 + c_9 u_{1,tt} = 0 \quad (8.1)$$

$$c_{10} N_1 + c_{11} N_{2,2} + c_{12} N_2 + c_{13} N_{12,1} + c_{14} N_{12} + c_{15} u_2 + c_{16} u_{3,2} + c_{17} \beta_2 + c_{18} u_{2,tt} = 0 \quad (8.2)$$

$$\begin{aligned} c_{19} N_1 + c_{20} N_2 + c_{21} u_{1,1} + c_{22} u_1 + c_{23} u_{2,2} + c_{24} u_2 + c_{25} u_{3,11} + c_{26} u_{3,1} + c_{27} u_{3,2} + c_{28} u_{3,2} \\ + c_{29} \beta_{1,1} + c_{30} \beta_1 + c_{31} \beta_{2,2} + c_{32} \beta_2 + c_{33} u_{3,tt} = 0 \end{aligned} \quad (8.3)$$

$$c_{34} M_{1,1} + c_{35} M_1 + c_{36} M_2 + c_{37} M_{12,2} + c_{38} M_{12} + c_{39} u_1 + c_{40} u_{3,1} + c_{41} \beta_1 + c_{42} \beta_{1,tt} = 0 \quad (8.4)$$

$$c_{43} M_1 + c_{44} M_{2,2} + c_{45} M_2 + c_{46} M_{12,1} + c_{47} M_{12} + c_{48} u_2 + c_{49} u_{3,2} + c_{50} \beta_2 + c_{51} \beta_{2,tt} = 0 \quad (8.5)$$

where t is time. It is noted that rotary inertia terms (with coefficients c_{42} and c_{51}) are included in Eqs. (8.4) and (8.5). The coefficients c_i are defined in terms of the material and geometric properties by

$$\begin{aligned}
c_1 &= -A_2; \quad c_2 = -A_{2,1}; \quad c_3 = -c_2; \quad c_4 = -A_1; \quad c_5 = -2A_{1,2}; \quad c_6 = b_{17} / R_1^2; \quad c_7 = -b_{17} / (A_1 R_1) \\
c_8 &= -b_{17} / R_1; \quad c_9 = A_1 A_2 \gamma h; \quad c_{10} = -A_1 A_2; \quad c_{11} = A_{1,2}; \quad c_{12} = c_4; \quad c_{13} = -c_{11}; \quad c_{14} = c_1 \\
c_{15} &= -2A_{2,1}; \quad c_{16} = b_{17} / R_2^2; \quad c_{17} = -b_{17} / (A_2 R_2); \quad c_{18} = -b_{17} / R_2; \quad c_{19} = c_9; \quad c_{20} = c_{10} \\
c_{21} &= A_1 A_2 / R_1; \quad c_{22} = A_1 A_2 / R_2; \quad c_{23} = -b_{18} A_2 / R_1; \quad c_{24} = b_{18} (A_2 / R_1)_{,1}; \quad c_{25} = b_{18} A_1 / R_2 \\
c_{26} &= b_{18} (A_1 / R_2)_{,2}; \quad c_{27} = -b_{18} A_2 / A_1; \quad c_{28} = -b_{18} (A_2 / R_1)_{,1}; \quad c_{29} = -b_{18} A_1 / A_2 \\
c_{30} &= -b_{18} (A_1 / A_2)_{,2}; \quad c_{31} = -b_{18} A_2; \quad c_{32} = -b_{18} A_{2,1}; \quad c_{33} = -b_{18} A_1; \quad c_{34} = -b_{18} A_{1,2} \\
c_{35} &= c_9; \quad c_{36} = c_{10}; \quad c_{37} = -c_1; \quad c_{38} = -c_2; \quad c_{39} = -c_2; \quad c_{40} = -c_{12}; \quad c_{41} = 2c_{11}; \quad c_{42} = -c_8 \\
c_{43} &= -b_{17} / A_1; \quad c_{44} = -b_{17}; \quad c_{45} = -A_1 A_2 \gamma h^3 / 12; \quad c_{46} = c_{13}; \quad c_{47} = -c_4; \quad c_{48} = c_{11} \\
c_{49} &= -c_1; \quad c_{50} = 2b_3; \quad c_{51} = b_{17} / R_2; \quad c_{52} = -b_{17} / A_2; \quad c_{53} = -b_{17}; \quad c_{54} = c_{45}
\end{aligned} \tag{9}$$

where γ is the mass density.

The further theory will be written for shells of revolution. The q_1 variable is taken then to represent the circumferential direction φ , and the q_2 variable the meridional direction θ . Adopting a modal approach, the displacement components and rotations are expanded in a Fourier series in the circumferential direction as

$$\begin{aligned}
u_1 &= u(\theta) \sin m\varphi \sin \omega t; \quad u_2 = v(\theta) \cos m\varphi \sin \omega t; \quad u_3 = w(\theta) \cos m\varphi \sin \omega t \\
\beta_1 &= \alpha(\theta) \sin m\varphi \sin \omega t; \quad \beta_2 = \beta(\theta) \cos m\varphi \sin \omega t
\end{aligned} \tag{10}$$

where m is the number of the circumferential harmonic, u , v , and w are the amplitudes of the displacements in the circumferential, meridional and normal directions for the m th harmonic, α and β are the amplitudes of the respective rotations, and ω is the circular frequency in rad/sec. Each harmonic may be analyzed separately, and the problem is thus reduced mathematically to one-dimension.

The equations of motion for shells of revolution can be represented as

$$e_1 u_{,22} + e_2 u_{,2} + (e_3 - m^2 e_4) u - m e_5 v_{,2} - m e_6 v - m e_7 u_3 + e_8 \alpha - e_9 \omega^2 u = 0 \tag{11.1}$$

$$-m e_{10} u_{,2} - m e_{11} u + e_{12} v_{,22} + e_{13} v_{,2} + (e_{14} - m^2 e_{19}) v + e_{16} w_{,2} + e_{17} w + e_{18} \beta - e_{19} \omega^2 v = 0 \tag{11.2}$$

$$\begin{aligned}
m e_{20} u + e_{21} v_{,2} + e_{22} v + e_{23} w_{,22} + e_{24} w_{,2} + (e_{25} - m^2 e_{26}) w + m e_{27} \alpha + e_{28} \beta_{,2} \\
+ e_{29} \beta - e_{30} \omega^2 w = 0
\end{aligned} \tag{11.3}$$

$$e_{31} u - m e_{32} w + e_{33} \alpha_{,22} + e_{34} \alpha_{,2} + (e_{35} - m^2 e_{36}) \alpha - m e_{37} \beta_{,2} - m e_{38} \beta - e_{39} \omega^2 \alpha = 0 \tag{11.4}$$

$$e_{40} v + e_{41} w_{,2} + m e_{42} \alpha_{,2} + m e_{43} \alpha + e_{44} \beta_{,22} + e_{45} \beta_{,2} + (e_{46} - m^2 e_{47}) \beta - e_{48} \omega^2 \beta = 0 \tag{11.5}$$

where the e_i are known coefficients expressible in terms of the geometric parameters and the a_i , b_i , and c_i coefficients given in this section. For each circumferential mode m , there are five field equations, in one geometric variable, for five unknown functions and the unknown frequency ω .

The $m = 0$ case, i.e., the axi-symmetric circumferential harmonic, is a special case that can easily be extracted from the theory for the general harmonic described in the preceding. In this special case, the displacement component u_1 , the rotation β_1 , and the resultants N_{12} , M_{12} , Q_1 will be zero, and the Eqs. (11.1) and (11.4) will become trivial.

4. Theory of elasticity

When the wall of the shell is considered thick, the assumption that a normal remains normal is no longer valid. For such shells, accurate results can be obtained using the theory of elasticity, which permits arbitrary variation of components in the thickness direction, and mathematically contains one additional position variable relative to shell theory. The consideration is again restricted here to linear behavior of shells consisting of elastic homogeneous isotropic materials.

In the theory of elasticity, the normal and shear strain components (Buchanan and Liu 2005, Redekop 1992) are

$$\begin{aligned}\varepsilon_1 \equiv \varepsilon_\phi &= a_1 u_{1,1} + a_2 u_2 + a_3 u_3; & \varepsilon_4 \equiv \varepsilon_{\theta\phi} &= a_6 u_{1,2} + a_7 u_1 + a_8 u_{2,1} \\ \varepsilon_2 \equiv \varepsilon_\theta &= a_4 u_{2,2} + a_5 u_3; & \varepsilon_5 \equiv \varepsilon_{r\phi} &= u_{1,3} + a_9 u_1 + a_{10} u_{3,1} \\ \varepsilon_3 \equiv \varepsilon_r &= u_{3,3}; & \varepsilon_6 \equiv \varepsilon_{r\theta} &= u_{2,3} + a_{11} u_2 + a_{12} u_{3,2}\end{aligned}\quad (12)$$

where u_1, u_2, u_3 are respectively the displacement components in the $q_1 \equiv \phi, q_2 \equiv \theta,$ and $q_3 \equiv r$ directions (Fig. 3), and the comma subscript again indicates differentiation with respect to the q_i variable that follows.

The coefficients a_i in the expressions for the strain components are defined for toroidal coordinates as

$$\begin{aligned}a_1 &= 1/\rho; & a_2 &= -\sin\theta/\rho; & a_3 &= \cos\theta/\rho; & a_4 &= 1/r; & a_5 &= a_4; & a_6 &= a_4 \\ a_7 &= -a_2; & a_8 &= a_1; & a_9 &= -a_3; & a_{10} &= a_1; & a_{11} &= -a_4; & a_{12} &= a_4\end{aligned}\quad (13)$$

where $\rho = R + r \cos\theta$, R is again the bend radius, and r is now the radial coordinate. The normal and shear stress components are given by

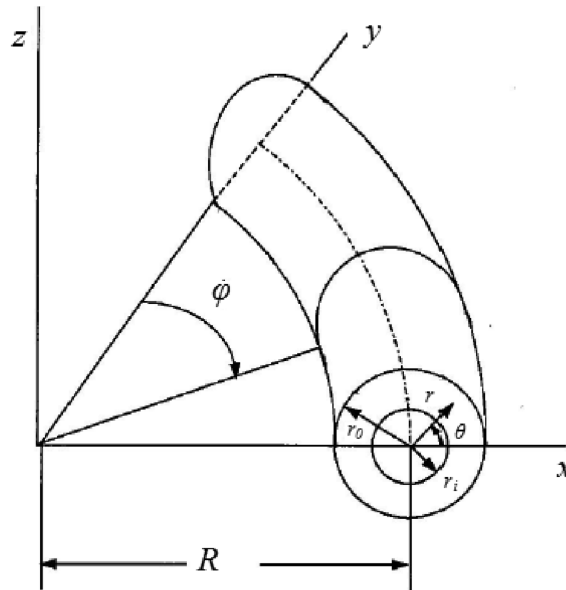


Fig. 3 Geometry and coordinates for analysis using theory of elasticity

$$\begin{aligned}
\sigma_1 \equiv \sigma_\phi &= b_1 \varepsilon_1 + b_2 \varepsilon_2 + b_3 \varepsilon_3; & \sigma_4 \equiv \sigma_{\theta\phi} &= b_{10} \varepsilon_4 \\
\sigma_2 \equiv \sigma_\theta &= b_4 \varepsilon_1 + b_5 \varepsilon_2 + b_6 \varepsilon_3; & \sigma_5 \equiv \sigma_{r\phi} &= b_{11} \varepsilon_5 \\
\sigma_3 \equiv \sigma_r &= b_7 \varepsilon_1 + b_8 \varepsilon_2 + b_9 \varepsilon_3; & \sigma_6 \equiv \sigma_{r\theta} &= b_{12} \varepsilon_6
\end{aligned} \tag{14}$$

The coefficients b_i are defined for homogeneous isotropic materials by

$$b_1 = b_5 = b_9 = K_1; \quad b_2 = b_3 = b_4 = b_6 = b_7 = b_8 = K_2; \quad b_{10} = b_{11} = b_{12} = K_3 \tag{15}$$

where $K_1 = 2(1 - \nu)G/(1 - 2\nu)$, $K_2 = 2\nu G/(1 - 2\nu)$, $K_3 = 2G$, and where E is again the Young's modulus, ν the Poisson's ratio, and $2G = E/(1 + \nu)$.

The equations of motion for a toroidal shell are given by

$$\begin{aligned}
c_1 \sigma_{1,1} + c_2 \sigma_{4,2} + c_3 \sigma_4 + \sigma_{5,3} + c_4 \sigma_5 &= \gamma u_{1,tt} \\
c_5 \sigma_1 + c_6 \sigma_{2,2} + c_7 \sigma_2 + c_8 \sigma_{4,1} + \sigma_{6,3} + c_9 \sigma_6 &= \gamma u_{2,tt} \\
c_{10} \sigma_1 + c_{11} \sigma_2 + \sigma_{3,3} + c_{12} \sigma_3 + c_{13} \sigma_{5,1} + c_{14} \sigma_{6,2} + c_{15} \sigma_6 &= \gamma u_{3,tt}
\end{aligned} \tag{16}$$

where γ is again the mass density. The coefficients c_i are defined for toroidal coordinates as

$$\begin{aligned}
c_1 &= 1/\rho; & c_2 &= 1/r; & c_3 &= -2\sin\theta/\rho; & c_4 &= (R + 3r\cos\theta)/r\rho; & c_5 &= \sin\theta/\rho \\
c_6 &= c_2; & c_7 &= -c_5; & c_8 &= c_1; & c_9 &= (2R + 3r\cos\theta)/r\rho; & c_{10} &= -\cos\theta/\rho \\
c_{11} &= -c_2; & c_{12} &= (R + 2r\cos\theta)/r\rho; & c_{13} &= -c_1; & c_{14} &= c_2; & c_{15} &= -c_5
\end{aligned} \tag{17}$$

Adopting again a modal approach, the displacement components are expanded in a Fourier series in the circumferential direction as

$$u_1 = u(\theta, r) \sin m\phi \sin \omega t; \quad u_2 = v(\theta, r) \cos m\phi \sin \omega t; \quad u_3 = w(\theta, r) \cos m\phi \sin \omega t \tag{18}$$

where m is the number of the circumferential harmonic, u , v , and w are the amplitudes of the displacements in the circumferential, meridional and normal directions for the m th harmonic, now functions of both θ and r , and ω is the circular frequency in rad/sec. Each harmonic may be analyzed separately, and the problem is now reduced mathematically to two-dimensions.

The equations of motion for a solid of revolution can be represented as

$$e_1 u_{,22} + e_2 u_{,2} + e_3 u_{,33} + e_4 u_{,3} + (e_5 - m^2 e_6)u - me_7 v_{,2} - me_8 v - me_9 w_{,3} - me_{10} w - \gamma u_{,tt} = 0 \tag{19.1}$$

$$\begin{aligned}
me_{11} u_{,2} + me_{12} u + e_{13} v_{,22} + e_{14} v_{,2} + e_{15} v_{,33} + e_{16} v_{,3} + (e_{17} - m^2 e_{18})v + e_{19} w_{,2} + e_{20} w_{,3} \\
+ e_{21} w_{,23} + e_{22} w - \gamma v_{,tt} = 0
\end{aligned} \tag{19.2}$$

$$\begin{aligned}
me_{23} u_{,3} + me_{24} u + e_{25} v_{,2} + e_{26} v_{,3} + e_{27} v_{,23} + e_{28} v + e_{29} w_{,22} + e_{30} w_{,2} + e_{31} w_{,33} + e_{33} w_{,3} \\
+ (e_{33} - m^2 e_{34})w - \gamma w_{,tt} = 0
\end{aligned} \tag{19.3}$$

where the e_i are known coefficients expressible in terms of the geometric parameters and the a_i , b_i , and c_i are coefficients given in this section. For each circumferential mode m , there are thus three field equations, in two geometric variables, for three unknown functions and the unknown frequency ω .

The Eq. (19) are to be applied to the interior points of the domain, whereas on the inner and outer surfaces the following boundary conditions apply: $\sigma_{31} = 0$, $\sigma_{32} = 0$, and $\sigma_{33} = 0$. It is to be realized

that computer times for an ELT analysis will greatly exceed those for an SDT analysis due to the additional dimension in the variables.

The $m = 0$ case, i.e., the axi-symmetric circumferential harmonic, is a special case that can again easily be extracted from the theory for the general harmonic described in the preceding. In this special case, the displacement component u_1 , and the stresses σ_1 , σ_4 , and σ_5 will be zero, and the Eq. (19.1) will become trivial. The solution of the equation sets (11) and (19) using the DQM is now considered.

5. Differential quadrature method

Application of the DQM allows for the conversion of the differential equations written for a particular harmonic m to a set of linear simultaneous equations (Shu 2000, Bert and Malik 1996). For the shear deformation problem, a one-dimensional grid of sampling points is defined along a meridian of the radial plane; while for the elasticity problem, a two-dimensional grid is defined on the cross-sectional area of the radial plane.

The derivative of a function in a given direction is replaced by the weighted sum of the values of the function at specified sampling points in a line following the given direction. For a generic function $f(x)$ of a single variable, the series used to replace the r th derivative of the function at the sampling point x_i is taken as

$$\left. \frac{d^{(r)}f(x)}{dx^r} \right|_{x_i} = \sum A_{ih}^{(r)} f(x_h) \quad (20)$$

where the $A_{ih}^{(r)}$ are the weighting coefficients of the r th order derivative in the x direction for the i th sampling point, $f(x_h)$ is the value of $f(x)$ at the sampling point position x_h . The number of sampling points in the x direction is denoted by M . For a generic function of two variables $g(x, y)$, the series for the $(r + s)$ th partial derivative at the sampling point x_i, y_j is taken as

$$\left. \frac{\partial^{(r+s)}g(x, y)}{\partial x^r \partial y^s} \right|_{x_i, y_j} = \sum A_{ih}^{(r)} \sum B_{jk}^{(s)} g(x_h, y_k) \quad (21)$$

where $B_{jk}^{(s)}$ and N describe the series for the y direction, and $g(x_h, y_k)$ is the value of $g(x, y)$ at the sampling point position x_h, y_k .

In the DQM, the weighting coefficients are determined a-priori for a pre-selected grid with the aid of selected trial functions. For the shear deformation analysis of the present geometry involving a complete meridian, a Fourier harmonic basis was used for the weighting coefficients (Bert and Malik 1996), and sampling points were equally spaced in the coordinate q_2 . For such a scheme, explicit formulas for the weighting coefficients $A_{ih}^{(r)}$ are available (Bert and Malik 1996). For the analysis of a complete toroidal shell using the theory of elasticity, a Fourier harmonic basis was used for the weighting coefficients in the meridional direction, and sampling points were equally spaced. In the radial direction q_3 , the Chebyshev-Gauss-Lobatto scheme was used (Bert and Malik 1996) with unequal spacing of points. For both schemes, the explicit formulas available (Bert and Malik 1996) were used.

Application of the quadrature rule (20) of the DQM to the differential equations of the shear deformation theory leads to a set of linear simultaneous equations. The set reduces to the form

$$\begin{aligned}
L_{11}u + L_{12}v + L_{13}w + L_{14}\alpha + L_{15}\beta + \gamma\omega^2u &= 0 \\
L_{21}u + L_{22}v + L_{23}w + L_{24}\alpha + L_{25}\beta + \gamma\omega^2v &= 0 \\
L_{31}u + L_{32}v + L_{33}w + L_{34}\alpha + L_{35}\beta + \gamma\omega^2w &= 0 \\
L_{41}u + L_{42}v + L_{43}w + L_{44}\alpha + L_{45}\beta + \gamma\omega^2\alpha &= 0 \\
L_{51}u + L_{52}v + L_{53}w + L_{54}\alpha + L_{55}\beta + \gamma\omega^2\beta &= 0
\end{aligned} \tag{22}$$

For the theory of elasticity it reduces to the form

$$\begin{aligned}
L_{11}u + L_{12}v + L_{13}w + \gamma\omega^2u &= 0 \\
L_{21}u + L_{22}v + L_{23}w + \gamma\omega^2v &= 0 \\
L_{31}u + L_{32}v + L_{33}w + \gamma\omega^2w &= 0
\end{aligned} \tag{23}$$

In either case, the matrix equation takes the form of the generalized eigenvalue problem

$$[\mathbf{K}](U) = \lambda[\mathbf{M}](U) \tag{24}$$

where the unknowns (U) are the values of the displacement functions at the sampling points, λ is the eigenvalue, related to ω , and $[\mathbf{K}]$, $[\mathbf{M}]$ are the known ‘stiffness’ and ‘mass’ matrices. Standard linear matrix routines may be used to solve the Eq. (24) for the eigenvalues and mode shapes.

6. Validation and results

The method is validated by comparing results from the SDT and ELT, for fifteen cases of complete toroidal shells, with results given in the literature. The geometric properties of the fifteen

Table 1 Properties of fifteen toroidal shell validation cases

Case	r_i	r_o	h	r_m	R	r_m/h	R/r_m	Material
1			0.001	0.0913	0.913	91.3	10	1
2			0.001	0.0645	0.645	64.5	10	1
3			0.001	0.0289	0.289	28.9	10	1
4			0.001	0.0204	0.204	20.4	10	1
5			0.001	0.00913	0.0913	9.13	10	1
6	0.9225	1.0775	0.1549	1	20	6.46	20	1
7	0.9225	1.0775	0.1549	1	10	6.46	10	1
8	0.9225	1.0775	0.1549	1	6.67	6.46	6.67	1
9	0.75	1	0.25	0.875	2.5	3.50	2.86	2
10	0.50	1	0.50	0.750	2.5	1.50	3.33	2
11	0.25	1	0.75	0.625	2.5	0.83	4.00	2
12			0.0025	0.25	1	100	4	1
13			0.0050	0.25	1	200	4	1
14			0.0050	0.50	1	100	2	1
15			0.0075	0.75	1	100	1.3	1

Table 2 Comparison of SDT frequencies ω_i (Hz) with PSE theory results of Kosawada *et al.* (1985) for thin shells - validation cases 1-5 ($m = 2$), (also quoted as cases 10-6 in Wang *et al.* (2006), Table 4)

Mode	Case 1		Case 2		Case 3		Case 4		Case 5	
	PSE	SDT	PSE	SDT	PSE	SDT	PSE	SDT	PSE	SDT
1	44.1	44.1	74.2	74.3	250	251	427	428	1344	1360
2	47.3	47.5	79.3	79.8	263	265	443	447	1353	1368
3	509.0	509.1	745.5	745.9	1840	1842	2827	2835	9247	9253
4	577.7	577.7	850.7	850.9	2076	2076	3156	3157	10043	10003
5	630.6	630.8	969.8	970.6	2993	2994	5316	5316	13428	13418
6	631.2	631.3	970.5	970.7	3000	2995	5331	5320	19720	19722

cases are given in Table 1, where r_i , r_m , and r_o represent respectively the inside, mean, and outside radius of the cross-section. It is seen that cases 1-5 are shells that have radius to thickness ratios r_m/h mostly greater than 10. Such shells are traditionally considered as thin. Cases 6-8 have an r_m/h ratio of about 6.5, and are considered moderately-thick shells. Cases 9-11 have an r_m/h ratio less than 4, and represent thick shells. Cases 12-15 again represent thin shells. The overall range in r_m/h ratio is from 91.3 to 0.83. The material properties used in the calculations are

$$\begin{aligned} \text{Mat.1: } E &= 0.207 \times 10^{12} \text{ Pa; } \nu = 0.3; \gamma = 7800 \text{ kg/m}^3 \\ \text{Mat.2: } E &= 0.193 \times 10^{12} \text{ Pa; } \nu = 0.291; \gamma = 7850 \text{ kg/m}^3 \end{aligned} \quad (25)$$

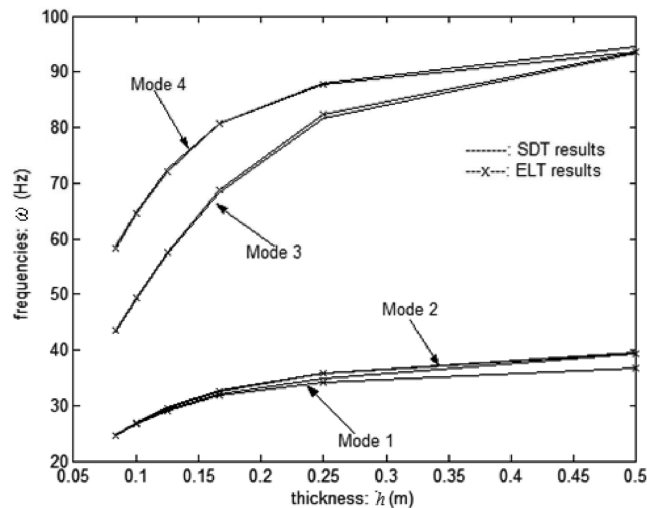
Results for the validation cases, given in Tables 2-6, and for the parametric study, given in Table 7, are for completely free support conditions. For the thin cases 1-5 covered in Table 2, the first six natural frequencies ω_i are given in Hz for the 2nd circumferential harmonic. For the moderately-thick cases 6-8 covered in Table 3, a similar set of frequencies ω_i in Hz is given. For the thick cases 9-11 covered in Table 4, the frequency parameters $\omega_i = \omega_i r_o \sqrt{2G}$ are given for the first six modes for the 2nd harmonic. For thin cases 12-15 covered in Table 5, the natural frequencies ω_i are given for the first six modes and for the axi-symmetric harmonic.

In Table 2, the PSE (power series expansion) values in Hz are taken from Wang *et al.* (2006), but stem from a thin shell analysis by Kosawada *et al.* (1985) (Table 3, p. 2047). The SDT results are determined using the shear deformation theory of section 3. For the five cases, there is agreement within 1.2% for the fundamental frequency as determined by the two methods. The largest difference occurs for the thickest shell (case 5). For the subsequent five frequencies, the agreement is nearly as good. The trend of the fundamental frequency from thinnest to thickest shell (case 1 to case 5) is clearly an increasing one, as would be expected for a set of shells having the same material properties and R/r_m ratio.

In Table 3, the TSL (thick shell Lagrangian) results are from Kosawada *et al.* (2006) (scaled from Fig. 3, p. 3041). Only the symmetric modes were represented in their study for these cases. The TSL theory corresponds to a shear deformation theory similar to the current one, but involves an awkward series solution in the thickness direction. The SDT results in Table 3 are from the present shear deformation theory, and the ELT results from the theory of elasticity of section 4. For the three cases, there is good agreement (mostly within 2%) for all six frequencies as determined by the three methods. The largest difference occurs in the shell with the smallest frequency, where the relative error due to scaling is the largest. The trend of the fundamental frequency from the shell with largest bend radius to shell with smallest bend radius (case 6 to case 8) is a significantly increasing one, as

Table 3 Comparison of SDT and ELT frequencies ω_i (Hz) with TSL theory results of Kosawada *et al.* (1986) for moderately-thick shell - validation cases 6-8 ($m = 2$)

Mode	Case 6			Case 7			Case 8		
	TSL	SDT	ELT	TSL	SDT	ELT	TSL	SDT	ELT
1	3.6	3.9	3.6	13.2	13.5	13.2	25.1	26.6	26.2
2	-	4.0	3.7	-	13.6	13.5	-	26.9	26.8
3	57.6	58.0	58.0	105.2	104.2	104.5	120.8	122.0	122.1
4	-	91.3	91.3	-	116.0	116.3	-	129.1	129.2
5	105.8	105.4	106.0	128.0	128.1	128.2	180.2	182.1	181.9
6	-	105.7	106.4	-	180.1	180.0	-	263.0	262.9

Fig. 4 Effect of change in thickness on frequency results for the case $R/r_m = 6$ Table 4 Comparison of non-dimensional SDT AND ELT frequencies Ω_i with FEM results of Buchanan and Liu (2005) (Table 6, p. 258) for thick shells - validation cases 9-11 ($m = 2$)

Mode	Case 9			Case 10			Case 11		
	FEM	SDT	ELT	FEM	SDT	ELT	FEM	SDT	ELT
1	0.2482	0.2491	0.2479	0.2568	0.2646	0.2567	0.2537	0.2814	0.2534
2	0.2857	0.2832	0.2854	0.2965	0.2871	0.2963	0.2975	0.2818	0.2973
3	0.5288	0.5243	0.5263	0.9762	0.9506	0.9759	1.0081	1.0072	1.0080
4	0.5396	0.5361	0.5371	1.0553	0.9676	1.0529	1.2172	1.2529	1.2172
5	0.9655	0.9633	0.9654	1.0782	1.0058	1.0758	1.7606	1.4237	1.7535
6	1.1137	1.1146	1.1134	1.1851	1.1946	1.1847	1.7729	1.4357	1.7655

would be expected for a set of shells having the same material properties and r_m/h ratio.

In Table 4, the FEM results are those given by Buchanan and Liu (2005), while the SDT and ELT results are again from the theories of sections 3 and 4. There is agreement within 1%, 3%, and 11%

Table 5 Convergence examples and comparison of SDT frequencies ω_i (rad/s) with results of Wang and Redekop (2005) (Table 4, p. 742) for thin shells - validation cases 12-15 ($m = 0$)

Mode/N	Case 12			Case 13			Case 14	Case 15
	10	40	100	10	40	100	40	40
1 ^a		383.4			553.4		279.2	245.9
1	499.0	389.6	389.6	598.8	562.5	562.5	283.8	249.9
2	3106	2686	2686	3144	2990	2990	2165	1869
3	3256	2779	2779	3444	3250	3250	2227	1917
4	3286	2808	2808	3469	3332	3332	2247	1926
5	4143	3033	3033	4327	3765	3765	2383	2042
6	4904	-	3447	5030	-	4071	-	2311

^a indicates result in Wang and Redekop (2005), Table 4, p. 742.

Table 6 Effect of rotary inertias and comparison of SDT frequencies ω_i (rad/s) with ELT results for moderately-thick and thick shells - validation cases 7-9 ($m = 0$)

Mode	Case 7			Case 8			Case 9		
	ELT	SDT/w ^a	SDT/wo ^b	ELT	SDT/w ^a	SDT/wo ^b	ELT	SDT/w ^a	SDT/wo ^b
1	49.8	49.7	49.7	63.0	62.6	62.6	148.8	145.2	145.2
2	82.0	81.9	81.9	118.5	118.4	118.4	271.6	269.5	269.5
3	118.0	117.5	117.5	141.1	140.9	140.9	369.5	368.6	368.6
4	121.2	120.7	120.7	147.6	147.4	147.4	405.0	404.2	404.2
5	288.8	286.4	286.4	296.6	294.4	294.4	619.9	608.3	608.3
6	288.8	286.4	286.4	296.6	294.5	294.5	620.5	609.3	609.3

^aSDT/w - rotary inertia effects included. ^bSDT/wo rotary inertia effects neglected.

Table 7 New results for SDT and ELT frequencies ω_i (Hz) for various R/r_m and r_m/h ratios, for material 1 (bracketed quantity indicates the circumferential harmonic number)

R/r_m	r_m/h	8		6		4		
		Mode	STD	ELT	STD	ELT	STD	ELT
2	1	1	88.2 (0)	89.1 (0)	105.2 (0)	106.7 (0)	136.0 (0)	139.5 (0)
	2	2	146.5 (2)	144.7 (2)	162.8 (2)	161.5 (2)	179.3 (2)	178.9 (2)
	3	3	176.4 (2)	173.8 (2)	207.2 (2)	204.6 (2)	215.5 (2)	217.9 (2)
	4	4	209.1 (2)	209.7 (2)	211.4 (2)	212.5 (2)	258.9 (1)	259.6 (1)
4	1	1	52.9 (2)	52.5 (2)	59.1 (2)	58.7 (2)	65.9 (2)	65.4 (2)
	2	2	55.8 (2)	55.5 (2)	62.7 (2)	62.7 (2)	70.5 (2)	70.8 (2)
	3	3	65.4 (0)	65.8 (0)	79.6 (0)	80.3 (0)	102.1 (0)	103.8 (0)
	4	4	117.3 (1)	117.3 (1)	131.9 (1)	132.2 (1)	158.1 (1)	158.8 (3)
6	1	1	29.3 (2)	29.0 (2)	32.0 (2)	31.7 (2)	34.9 (2)	34.2 (2)
	2	2	29.6 (2)	29.5 (2)	32.7 (2)	32.6 (2)	35.9 (2)	35.8 (2)
	3	3	57.3 (0)	57.6 (0)	68.3 (0)	68.8 (0)	81.7 (0)	82.4 (0)
	4	4	72.5 (3)	72.1 (3)	80.8 (3)	80.6 (3)	87.9 (3)	87.7 (3)

for the fundamental frequency of case 9-10 as determined by the FEM and STD methods. The largest difference occurs for the thickest shell (case 11). For the other five frequencies, the agreement is even better. The agreement of the FEM and ELT results is within 1% for all cases and modes. The trend of the fundamental frequency from thinnest to thickest shell (case 9 to case 11) is a very modestly increasing one. It is seen that although the R/r_o is constant for these cases, the R/r_m ratio is not. Overall, the results of Tables 2-4 indicate that the SDT shows close agreement with other applicable theories for an r_m/h ratio ranging from about 100 to 3.

Results given in Tables 5, 6 indicate further mathematical and physical characteristics of the SDT and ELT solutions. In Table 5, an indication is given for the convergence characteristics of the SDT results, and the accuracy of the axi-symmetric version of the theory. The comparison is with results for thin shells given earlier by Wang and Redekop (2005) (Table 4, p. 742). It is seen that three to four figure accuracy is given with a mesh of some 40 points in the DQM, for the lowest six frequencies. The agreement in the fundamental frequency with the previous thin shell theory results is within about 3%.

In Table 6, an indication is given of the significance by including the rotary inertia terms of the equations of motion of the SDT, and the accuracy of the axi-symmetric version of the ELT. The results given are for moderately-thick and thick shells (cases 7-9). It is seen that for these shells neglecting the rotary inertia terms does not affect the figures of accuracy cited. The agreement of the fundamental frequencies of the axi-symmetric versions of the SDT and ELT approaches is within 2%.

Free vibration frequencies are determined for nine more cases using complete isotropic toroidal shells as described in Table 7. For this parametric study, the range in the radius to thickness ratio r_m/h is from 8 to 4, and the range in the radius ratios R/r_m is from 2 to 6. The results for the first four frequencies from the SDT and ELT approaches are given in Hz, and the number of the mode in each case is given in brackets. It is seen that in this parametric range, the contribution to the fundamental frequency either comes from the axi-symmetric or 2nd circumferential harmonic, and that further contributions within the first four frequencies come from the 1st and 3rd harmonics. It is observed that there is close agreement between the two theories, and that as r_m is kept constant,

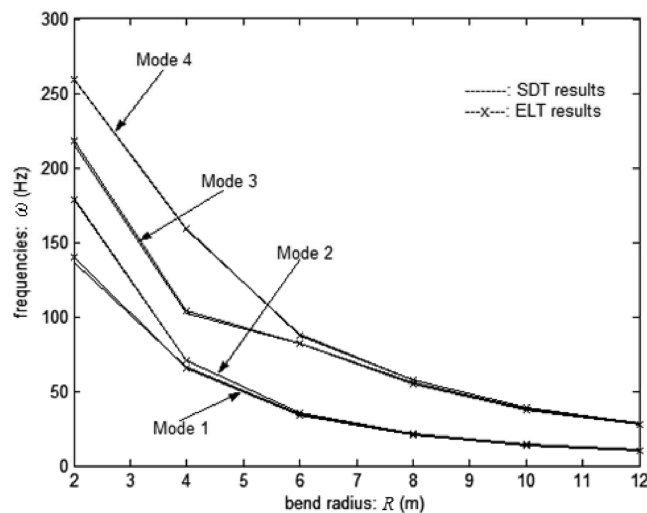


Fig. 5 Effect of change in bend radius on frequency results for the case $r_m/h = 4$

the frequencies increase as the thickness is increased, and decrease as the bend radius is increased.

These trends are further illustrated by two examples shown in Figs. 4 and 5. Fig. 4 shows, for the case $R/r_m = 6$, the trends of the frequencies of the first four modes as the thickness is increased. Fig. 5 shows, for the case $r_m/h = 4$, the trends of the frequencies for the first four modes as the bend radius is increased. The two figures again demonstrate the close agreement of SDT and ELT results.

7. Conclusions

General equations intended to predict the natural frequencies of moderately-thick toroidal shells have been presented based on the shear deformation theory of Soedel. Further equations based on the theory of elasticity have been presented for application to thick toroidal shells. Results from the two sets of equations are consistent with previously published results. It is demonstrated that the shear deformation theory gives good results in the radius to thickness range of 100 to 3. Results of a parametric study for the natural frequencies of moderately-thick and thick toroidal shells are given. The study demonstrates the value of the shear deformation theory for the vibration analysis of circular toroidal shells.

Acknowledgements

This work was supported by the Initial Research Funding of Shantou University (Grant no. 091065).

References

- Artioli, E., Gould, P.L. and Viola, E. (2005), "A differential quadrature method solution for shear-deformable shells of revolution", *Eng. Struct.*, **27**, 1879-1892.
- Artioli, E. and Viola, E. (2006), "Free vibration analysis of spherical caps using a GDQ numerical solution", *ASME J. Press Vessel Technol.*, **128**, 370-378.
- Balderes, T. and Armenakas, A.E. (1973), "Free vibrations of ring-stiffened toroidal shells", *AIAA J.*, **11**(2), 1637-1644.
- Bert, C.W. and Malik, M. (1996), "Free vibration analysis of thin cylindrical shells by the differential quadrature method", *ASME J. Press Vessel Technol.*, **118**, 1-12.
- Buchanan, G.R. and Liu, Y.J. (2005), "An analysis of the free vibration of thick-walled isotropic toroidal shells", *Int. J. Mech. Sci.*, **47**, 277-292.
- Jiang, W. and Redekop, D. (2002), "Polar axisymmetric vibration of a hollow toroid using the differential quadrature method", *J. Sound Vib.*, **251**(4), 761-765.
- Kosawada, T., Suzuki, K. and Takahashi, K.S. (1985), "Free vibrations of toroidal shells", *Bull. JSME*, **28**(243), 2041-2047.
- Kosawada, T., Suzuki, K. and Takahashi, S. (1986), "Free vibrations of thick toroidal shells", *Bull. JSME*, **29**(255), 3036-3042.
- Leung, A.Y.T. and Kwok, N.T.C. (1994), "Free vibration analysis of a toroidal shell", *Thin Wall. Struct.*, **18**, 317-332.
- McGill, D.F. and Lenzen, K.H. (1967), "Polar axisymmetric free oscillations of thick hollowed tori", *SIAM J. Appl. Math.*, **15**(3), 679-692.
- Redekop, D. (1992), "A displacement approach to the theory of toroidal elasticity", *Int. J. Pres Ves Pip.*, **51**(2),

189-209.

Shu, C. (2000), *Differential Quadrature and Its Application in Engineering*, Springer-Verlag, Berlin.

Soedel, W. (1982), "On the vibration of shells with Timoshenko-Mindlin type shear deflections and rotary inertia", *J. Sound Vib.*, **83**(1), 67-79.

Soedel, W. (2004), *Vibration of Shells and Plates*, 3rd. Edition, Marcell Decker, New York.

Wang, X.H. and Redekop, D. (2005), "Natural frequencies and mode shapes of an orthotropic thin shell of revolution", *Thin Wall. Struct.*, **43**, 735-750.

Wang, X.H., Xu, B. and Redekop, D. (2006), "Theoretical natural frequencies and mode shapes for thin and thick curved pipes and toroidal shells", *J. Sound Vib.*, **292**, 424-434.